

Development of a Modular Link for Colonoscopy Intubation

Kaiqiang Liu

Ohio University, Mechanical Engineering, Athens, Ohio, U.S.A.

Email: kl881812@ohio.edu

JungHun Choi

Georgia Southern University, Mechanical Engineering, Statesboro, Georgia, U.S.A.

Email: jchoi@georgiasouthern.edu

Abstract— A shape adjusting modular robotic system was implemented to improve the colonoscopy intubation process. The system consists of independent and homogenous robotic modules. Each individual module has its own processor, actuators, sensors, power supply, Bluetooth module, and unique end-effector. Modules are capable of sending and receiving data wirelessly via Bluetooth in order to communicate between modules. The number of modules in the system and the end-effectors can be varied to complete different tasks. A prototype was built with three modules connected in series in order to replace the colonoscope's distal tip and semi autonomously navigate the colon while being passively advanced. The BT communication protocol is defined, the kinematics for the 5-degree-of-freedom robotic system is modeled, and the shape changes were simulated in MATLAB. Performance of the system was tested on an up-scaled sigmoid colon model, which resulted in effective collision avoidance between its body and the colon wall.

Index Terms—colonoscopy, robotics, bluetooth communication, intubation, forward/inverse kinematics

I. INTRODUCTION

As robotic technologies have developed in recent years, more possibilities of applying robots to the medical field have arisen. Robotic development in the field of colonoscopy can aid in eliminating the limitations of the current procedure: namely, the invasive nature of the procedure and the necessity of a high skilled and experienced doctor [1]. Colon and rectum diseases such as hemorrhoids, diverticular disease, irritable bowel syndrome (IBS), ulcerative colitis and colorectal cancer are very common worldwide. Furthermore, the number of patients is increasing rapidly with over 1 million new colorectal cancer cases found in the world every year [2]. Colonoscopy is by far the most common and effective way to detect and treat colon and rectum diseases mentioned above [3, 4]. People at the age of 50 or above are encouraged to undergo a colonoscopy every 10 years. Furthermore, increased screening is recommended if the patient has personal history of polyps or risk factors other

than age [5]. The colonoscope itself has a significant rigidity. The last 10 cm of the shaft is called the distal tip of the colonoscope. It can bend up, down, left, and right when manipulated by the doctor through the control head. Once the tip of the scope stalls and the rest of it are still being inserted into the body, it will form a loop and stretch the colon because of the stiffness of the scope and the lack of fixation of the colon (especially the sigmoid colon). This can cause a severe discomfort to the patient as well as serious complications such as clinic perforation [6-8].

To overcome the discomfort and make the colonoscopy procedure more safe, robotic modules can be applied [9]. There are certain challenges that exist in the development of a modular robotic system that is able to solve problems in colonoscopy, such as the invasion nature of the procedure and the dependence of a highly skilled and experienced doctor. These challenges can be broken down into three aspects: the wireless communication capability for multiple modules for more flexibilities, the difficulties in building the mathematical models, and the hardware limitations regarding the degree of freedom and actual dimension. Most of the current modular robots use wires or hardware based electrical interface for communication, which limits the flexibility and independence of the robot.

Thus, a modular snake-like robotic system has been developed in order to improve the colonoscopy procedure. Compared to a biological snake, the number of joints has been reduced and each module has been given a higher range of motion, and Bluetooth capability. The snake-like robotic system aims to ease the advancement of the colonoscope inside the colon by avoiding collision between the system's body and the colon wall, and, therefore, making the procedure less skill-dependent and friendlier to patients [10]. Each module usually has primary components such as a processor, actuator, as well as unique parts such as end-effectors and sensors for different tasks. Therefore, a modular robot can be versatile, especially when the task is not fully laid out in advance. In addition, modular robotic system can lower the cost of the overall robot since only one or few types of modules need to be made [10-12], or replaced when

one module is inoperative. Furthermore, the modules can have more functions when wireless communication capability is enabled, which allows remote manual intervention.

II. METHODS

A. Hardware

The system should be able to adjust its shape in 3-dimensions, so at least 3 distance sensors are needed to locate the position of each module. Thus, the dimension of the modules and all the components were preliminarily determined. The processor used in this research is Arduino Micro, which is an ATmega32u4 based microcontroller. The overall dimension of the board is $48 \times 18 \times 10$ mm ($1.9 \times 0.7 \times 0.4$ inches), including the pins for fitting in the breadboard. The Bluetooth module used in this research is Bluetooth Mate Silver and the dimension is $44 \times 16 \times 3$ mm ($1.75 \times 0.65 \times 0.12$ inches). The sensor used in this research is QRD1114 Reflective Object Sensor. The effective working distance is from 5 to 25 mm, which is adequate for function. Experimentation was set up to measure the relation between the distance and the reading using Arduino. The servo motors used are Hitec HS-55 Feather DC Servo motor. There are three modules (distal module, middle model and proximal module) will henceforth be referred to as Module 1 (M1), Module 2 (M2) and Module 3 (M3), respectively. There are two servos in each module connected vertically to each other. These will be referred to as the top one and the bottom one, respectively. The bottom one rotates about the longitudinal axis (yaw joint) and the top one rotates about the axis that is vertical to it (roll joint). The servos also come with horns, which can be connected to the shaft of the servo for mounting purposes. For kinematic reason, M1 was connected reversely (bracket to bracket with M2).

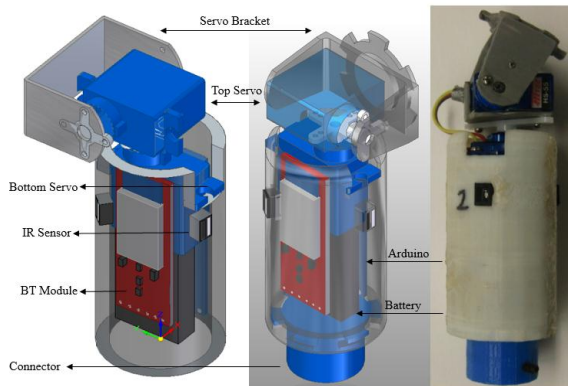


Figure 1. CAD model and pictures of the module, from left to right, the first prototype, the second one and the pictures of the module

From Fig. 1, the cylindrical outer casting houses the controller, battery, Bluetooth module, sensors, and the bottom servo motor. The top servo with the bracket is located outside the cylindrical cover. The configuration of the servos allows each module to have two degrees of freedom (pan and tilt). Each servo can rotate from 0 to

180, with 90 being the neutral position. There are three sensors around the circumference of the cylinder. The connector at the bottom connects a rubber insertion tube to the system. The integrated robotic system with three modules is shown in Fig. 2.

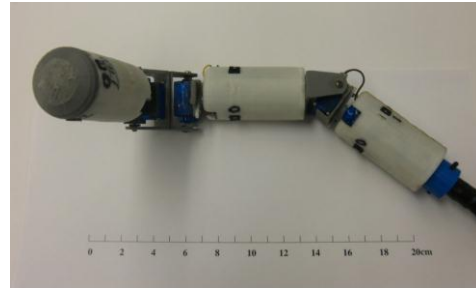


Figure 2. Prototype with three modules

B. Initial Configuration Setup

The initial configuration setup of the robotic system is the determination of the orientation of the sensors, the initial angles of the servos, and the angular relation between sensors and servos when taking the actual testing model into consideration. Although a real human colon is a 3D structure, the main turns of the colon stay in the coronal plane (frontal) of human body. Loops and collapses cause overlaps of the colon in midsagittal plane (medium). The robotic system needs to have a dominated turning direction that is convenient to control and competent for the sharp turns. The robotic system is connected in a yaw-to-roll manner. The roll joints can adjust the shape independently while the yaw joints only cooperate with the roll joints to adjust the shape. The robotic system should be initially set in a configuration in which the axes of the roll joints are vertical to the plane where the main turns of the testing model are at. In this way, the dominated turning direction is in the same plane as the turns are. Since the turns happen frequently, the control of the dominated turning motion should be as simple as possible. One of the sensors was initially placed in the dominated bending direction. Assuming that the cross section of the model is a circle, and it is parallel to the cross section of the sensor plane of the module, the schematic of the initial set up of the system is shown in Figure 3. When A_0 is triggered, the rolling joints can directly bend to adjust the shape.

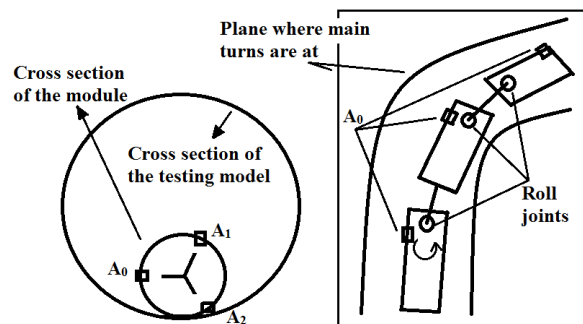


Figure 3. Schematic of the initial configuration setup

C. Bluetooth Communication

To adjust the shape of the robotic system, modules need to cooperate. For example, M1’s position can be adjusted by M2’s servo motor according to M1’s sensor input and servo motor position. Data need to be transmitted in a timely manner between 3 modules for the real time operation. The protocol of the currently used BT module dictates that a host, also called a “master device”, can send and receive data from only one active Bluetooth device, also called the “slave device”, at once. All of the Bluetooth devices on the external PC are serving as master devices. They initialize the connection between the modules one by one. After all the data “channels” (serial ports) are open, the PC is ready to send and receive data to each module respectively through three different serial ports. The schematic is shown in Fig. 4.

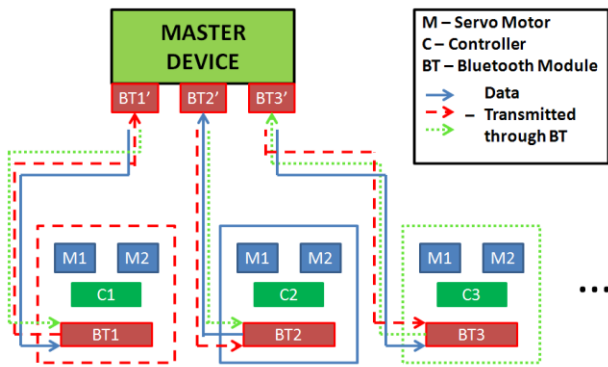


Figure 4. Schematic of the BT data transmission

The next step is to exchange the data between the robotic modules. To exchange the data, and send other data to the modules, there are two possible ways: 1. Develop program to control each of the serial communication individually and use other software to control these programs. 2. Develop one program to manage three serial communications. The first one can send and receive data simultaneously since they are three different programs. The time of each step is well adjusted so that every processor has enough time to finish their mission before the next one is due. Figure 5 shows the data transmission diagram.

D. Forward Kinematics

Denavit - Hartenberg (DH) Parameters [13] are a standard description of the geometric configuration of joints and links in a serial robot. The structure with each frame laid out under this assumption is shown in Fig. 6. The transformation matrix starts at the base (B) and ends at the end-effector, which is the center of the circle in which M1’s sensors are located on this forward kinematic analysis stage. There are 6 degrees of freedom in the system theoretically, but only 5 of them are in use of adjusting the position of the system. The DH parameters are listed in Table I. Counterclockwise is defined as positive direction in rotation.

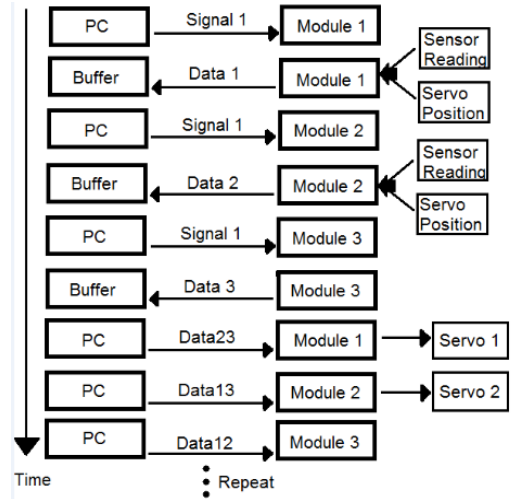


Figure 5. Data transmission diagram

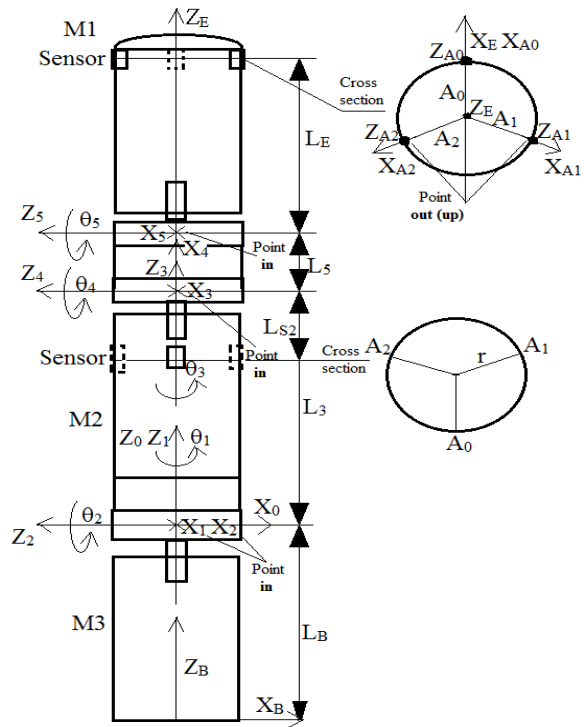


Figure 6. DH Parameters figure with intermediate frames

TABLE I. DH PARAMETERS OF THE ROBOTIC SYSTEM

i	α_{i-1}	a_{i-1}	d_i	θ_i
B	0	0	L_B	0
1	0	0	0	$90+\theta_1$
2	90	0	0	θ_2
3	-90	0	L_3	θ_3
4	90	0	0	$90+\theta_4$
5	0	L_5	0	$-90+\theta_5$
E	-90	0	L_E	0

The homogenous matrix ${}^{i-1}_i T$ is used to describe the transformation between neighboring frames. The formula is:

$${}^{i-1}T_i = \begin{bmatrix} \cos \theta_i & -\sin \theta_i & 0 & a_{i-1} \\ \sin \theta_i \cos \alpha_{i-1} & \cos \theta_i \cos \alpha_{i-1} & -\sin \alpha_{i-1} & -d_i \sin \alpha_{i-1} \\ \sin \theta_i \sin \alpha_{i-1} & \cos \theta_i \sin \alpha_{i-1} & \cos \alpha_{i-1} & d_i \cos \alpha_{i-1} \\ 0 & 0 & 0 & 1 \end{bmatrix} \quad (1.1)$$

Substituting each row of the DH parameters table into equation (1.1) yields all transformation matrices: ${}^{i-1}T_i$ ($i=1,2,3,4,5$), ${}^B T$ and ${}^E T$. Multiplying all consecutive transformation matrices yields the base to end transformation matrix, ${}^B T$:

$${}^B T = [{}^B T][{}^0 T][{}^1 T][{}^2 T][{}^3 T][{}^4 T][{}^5 T] \quad (1.2)$$

A stick model is built in MATLAB to simulate the position of the robotic system with respect to different joint angles.

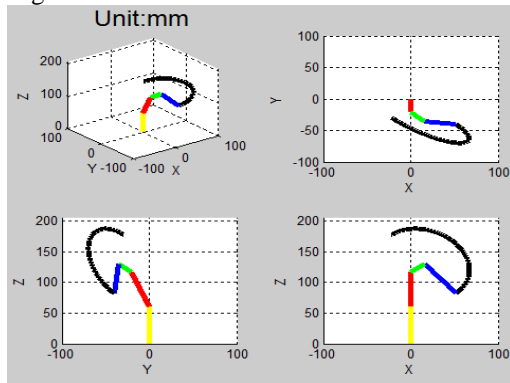


Figure 7. Stick model of the robotic system

In Fig. 7, 5 small segmental parts are M3, M2, link between M1 and M2, M1, and the trajectory of the end (E) with $\theta_1 = 0^\circ$, $\theta_2 = 20^\circ$, $\theta_3 = 60^\circ$, $\theta_4 = 45^\circ$, and θ_5 goes from -90° to 90° (0° to 180° in real pictures). Figure 8 is the real picture with the same joint angles, from left to right $\theta_5 = 0^\circ, 60^\circ, 120^\circ$ and 180° ($-90^\circ, -30^\circ, 30^\circ$, and 90° in stick model). The forward kinematic analyses help verify the position of the system with any joint angles and better understand the motion. More importantly, it is able to calculate the position and orientation (pose) of any single joint with all angles known. For the shape adjustment task, one joint will be isolated from others and placed into the desired position according to the sensor readings. The pose of the target position will be described using forward kinematics. After that, the pose is used in inverse kinematics to get the target joint angles.

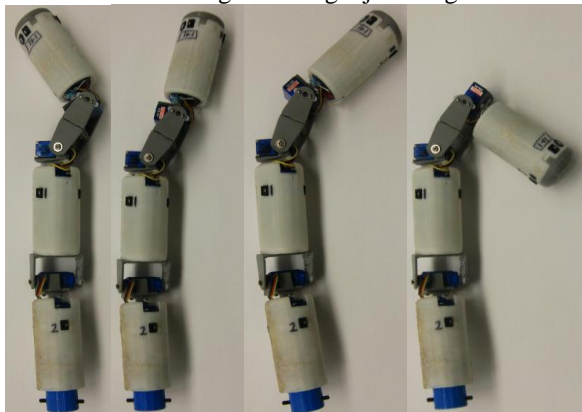


Figure 8. Real pictures of the robotic system with same joint angles used in the stick model

TABLE II. DH PARAMETERS TABLE FOR TRANSFORMATION FROM E TO A0, A1 AND A2

i	α_{i-1}	a_{i-1}	d_i	θ_i
E	-90	0	L_E	0
A ₀	0	r	$L_{A0i}-L_E$	0
-A ₀	0	-r	$L_{A0i}-L_E$	0
E	-90	0	L_E	-120
A ₁	0	r	$L_{A1i}-L_E$	0
-A ₁	0	-r	$L_{A1i}-L_E$	0
E	-90	0	L_E	120
A ₂	0	r	$L_{A2i}-L_E$	0
-A ₂	0	-r	$L_{A2i}-L_E$	0

E. Inverse Kinematics

The base of the system (the bottom of M3) is being advanced discretely, step by step. Once the system gets to a new position, it stops and executes one position adjustment loop. The inverse kinematics is being applied to every single loop. In each loop, the base is assumed to be fixed. By controlling the step length of each advancing of the system, the motion can be smooth and macroscopically continuous. Secondly, as the exact target position is very hard to be determined, a very unique and efficient way is used corresponding with the sensor system to define the target position [14, 15]. The shape is adjusted by setting “imaginary target position” according to the sensor readings, and moving the end (E) toward the direction of the “imaginary target position”. Recall the DH parameter diagram, the last point of the model is the end (E), which is the center of the circle, in which the sensors are, instead of each sensor. Now, the new DH parameters of frame E to A₀, A₁ and A₂ on M1 are introduced, shown in Table II.

As seen in Table II, θ (the angle between X axis of frame 5 and frame E according to Z_E) is the only DH variable that changes with respect to A₀, A₁ and A₂. Now, ${}^{E} T_{A_i}$ is introduced, and thus it yields the transformation from base (B) to imaginary sensor positions ($\pm A_0, \pm A_1$ and $\pm A_2$):

$${}^B T_{A_i} = [{}^B T][{}^0 T][{}^1 T][{}^2 T][{}^3 T][{}^4 T][{}^5 T][{}^E T_{A_i}] \quad (i=0,1,2) \quad (1.3)$$

At a certain position, ${}^E T_{A_i}$ can be calculated, and it is set as the target position bases on which sensor is triggered. Notice that there are $L_{A_{ji}}$ ($j=0, 1, 2$) and r in Table II. They are “imaginary height” (vertical distance between joint 5 and imaginary target position) and “imaginary length” (horizontal distance between joint 5 and imaginary target position) of the “imaginary target position”.

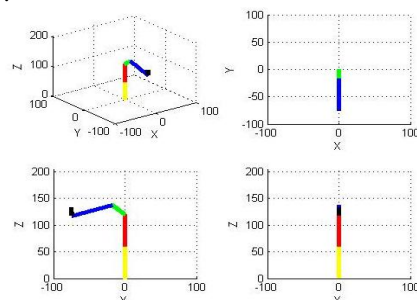


Figure 9. Stick model of the modular robot

In the model shown in Fig. 9, $\theta_1 = 0^\circ$, $\theta_2 = 0^\circ$, $\theta_3 = 0^\circ$, $\theta_4 = 45^\circ$, $\theta_5 = 64.3^\circ$. The black line segment is the “imaginary stick” between end (E) and the target position. In this case, r and L_{A0i} are chosen to be 15 and 55 mm (in Table 2, $a_{i-1} = 15$, $d_i = -5$). The r chosen here is much higher than it should be to safely get the solution, as the larger it is, the higher the chance that the target position will be out of the reachable area. The only reason here is to make it more visible so that it can be compared to the configuration at instant 2 (after executing the adjustment loop). Now the pose of the target position (A_0) is known. Move the end (E) to the target position (A_0) and solve for the joint angles.

$${}^B_E T = {}^B_{A20} T \quad (1.4)$$

$${}^B_5 T_{\text{numerical}} = {}^B_E T [{}^E_5 T] = {}^B_E T [{}^5_E T]^{-1} \quad (1.5)$$

From forward kinematics, ${}^B_5 T_{\text{analytical}}$ can be expressed in terms of joint angles, by equating them, yields:

$${}^B_5 T_{\text{numerical}} = {}^B_5 T_{\text{analytical}} \quad (1.6)$$

In this case, $\theta_1, \theta_2, \theta_3$ are all given values (only θ_4 and θ_5 are variables in ${}^B_5 T_{\text{analytical}}$), there are several reasons. For most of the positions, the robot is a kinematically redundant system. Opening all five degrees of freedom can easily cause an under determination of the solution. The movement can be optimized by trajectory generation. As a shape adjustment mechanism, the target position is better to be achieved with the least number of joints participated. Because motion from joint 1 and 2 will cause bigger change (can be desirable or undesirable) in position of M1, which plays the primary role in the shape adjustment task. The position of M1 is adjusted by both itself and M2 (joint 3, 4, 5), while M2’s position can only be adjusted by M3 (joint 1 and 2). Keep joint 1 and 2 independent with joint 3, 4 and 5 (give θ_1 and θ_2 values) when solving for θ_3, θ_4 and θ_5 can save a lot of operations (will be explained in the determination of the position of M2). By solving equation (1.6), two sets of solutions are obtained:

$$\begin{aligned} \theta_1 = 0^\circ, \theta_2 = 0^\circ, \theta_3 = 0^\circ \\ \theta_4 = 36.5547 \quad \text{and} \quad \theta_4 = -237.3363 \text{ or } 122.6637 \\ \theta_5 = 59.5819 \quad \theta_5 = -59.5819 \end{aligned}$$

The second set of solution is out of the servo’s range of motion. M1 is moved to the target position (large movement) only in this case just to show how it works, in read cases, the module will be moved a small step toward that direction. To fully adjust the shape, the position of M2 needs to be controlled, by M3 only, too. Theoretically, M2 should be adjusted before M1, and therefore analyzed before M1. However, the shape adjustment of M2 has several constraints in this case. Use the same method to get the target position for M2. Let θ_{2i} ($i = 1, 2$, first subscript “2” indicates M2, second one indicates joint 1

or 2) be the target position of M2, θ_i ($i = 3, 4, 5$) be the target position of M1. First solve for θ_{2i} ($i = 1, 2$). Set ${}^B_{A20} T$ (A_{20} is sensor A_0 on M2, ${}^B_{A20} T$ is the base to A_{20} transformation matrix) as the target position, yields:

$${}^B_3 T = {}^B_{A20} T \quad (1.7)$$

$${}^B_3 T = {}^B_3 T_{\text{analytical}} = {}^B_3 T_{\text{numerical}} = {}^B_{A20} T \quad (1.8)$$

By solving equation (1.8), θ_{2i} ($i = 1, 2$) is obtained. Then substitute θ_{2i} ($i = 1, 2$) into equation (1.6) and solve for θ_i ($i = 3, 4, 5$).

F. Integrated Working Principle

The real working principle is slightly different from the theoretical one that suggested by the kinematics analysis. All the programming for the modules is under the environment of Arduino, which is an open-source C/C++ based software. It is easy to access with low cost and convenient for troubleshooting. The data flow protocol is programmed in Python.

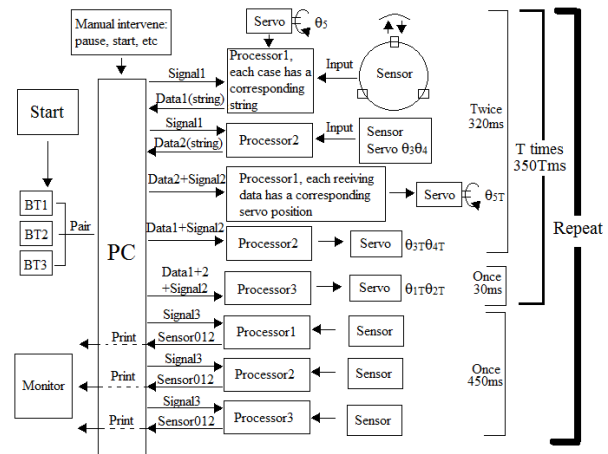


Figure 10. Overall working principle flow diagram

The overall working principle flow diagram is shown in Fig. 10. There are three types of signal from the PC: Signals 1, 2 and 3. Signal 1 asks for data from Arduino, Signal 2 tells the Arduino to move the servos. Signal 3 asks the Arduino for the exact sensor readings (float numbers), and the PC prints them out to the Python command window after receiving them to keep track of the sensor data. They are all strings followed by an end character. The Arduino reads the string bit by bit and it starts to process when it sees the end character. The data are sensor readings and servo positions.

G. Movement and Advancing Speed

As one of the criteria of the trajectory of each module, the robotic system is expected to move in a smooth and continuous pattern rather than to move large angles quickly, which could cause damage to the environment (the colon) and the system itself. The minimum increment of the servo motor is 1 degree. Within 1 degree, the speed is not controllable (built-in with the servo, theoretically

length is about 90 cm. It has features in three dimensions [16].

Since the insertion process were done manually, variations between trials were inevitable. Certain protocol was stipulated to minimize the variation brought in by the performer. The performer would run the test till enough knowledge of the process and stability was acquired before the actual experiment. A mark would be put on the entrance of the model so that every time the rubber shaft is inserted from the same position. The rubber insertion tube would be held firmly so that it would not move with the system.



Figure 12. Alpha loop and Testing Model [17]

III. RESULTS

The time was recorded every 13 cm of insertion for the first 26 cm of insertion. After 26 cm, the time was recorded every 10 cm of insertion until the completion of the process. The robotic system measures 26 cm when it is straight. So, the insertion length starts from -26 cm if the tip of the rubber tube is counted as 0 cm. Figure 13 shows the insertion time, the standard deviation (SD), and the coefficient of variation (CV). As CV is actually a dimensionless factor, it was multiplied by 10 in order to make it more visible in the graph and convenient for comparisons. The average total insertion time is 48.6 s and the standard deviation is 4.72 s.

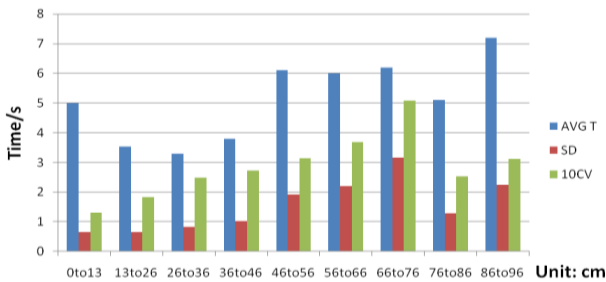


Figure 13. Average Insertion time, standard deviation and coefficient of variation of the 10 trials on Testing Model

Fig. 14 shows the real time pictures of the insertion process. Stick models were drawn in MATLAB with the servo positions feedback. The colored solid lines in the pictures are the imagined ideal position of the system for the insertion process. It is convenient for comparing with the stick model.

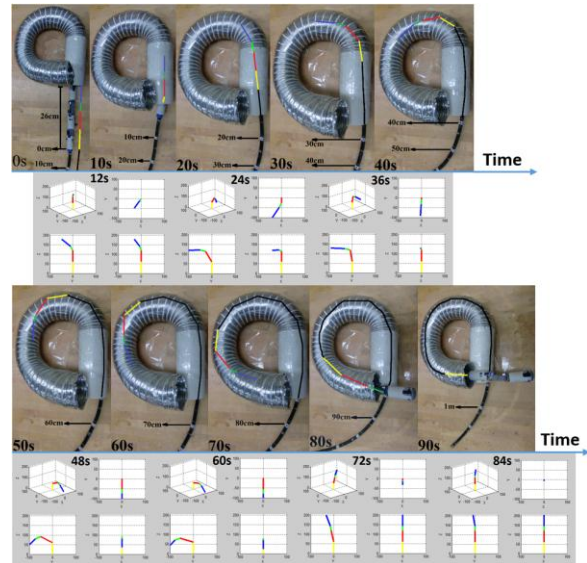


Figure 14. Real time pictures and Matlab stick models of the insertion process

The time is generally longer than the time recorded in those 10 trials mention above. It is because the process was slowed down to acquire more sensor feedback and pictures. The Y-Z plane projection of the stick model (lower left quarter) best describe the shape, as most of the turns of the model are in that plane. The X-Y plane projection (upper right quarter) reflects the rotation. In the 90s real picture (second row, 5th), it can be seen that about 90cm of the rubber shaft was inserted into the model. The robotic system measures 26cm in a straight configuration. The part that exposed out of the model measures about 18cm. Roughly 98 cm (system plus rubber tube) was inserted into the model before the distal tip of the system came out of the model.

Fig. 15 (a) and (b) show the sensor feedback of M1 and M2 for trial 1 on Testing Model. In Figure 15 (c), A_1 fluctuates above certain high value. Most of the fluctuations are above 3.0 except for 1 point. A_2 fluctuates between 0.2 and 4.5 frequently and dramatically. A_0 stays close to 0 for about 15s. From the stick model, it can be seen that during that period of time (about 48 to 60s), the roll joint of M3 (θ_2) was close to its angle limit (160° or above). However, no significant static force was experienced this time. Figure 15 (c) and (d) show the sensor feedback of M1 and M2 for trial 2 on Testing Model. A_1 stays above certain high value as expected. A_0 behaves similar as in the first trial. A_2 shows a trough with 2 continuous low points. In Figure 18, A_1 fluctuates slightly above certain high value. A_0 and A_2 fluctuate dramatically between 0 and 4.5. No continuous low points are shown. No significant difficulties were experienced during the process. Fig. 15 (e) and (f) show the sensor feedback of M1 and M2 for trial 3 on Testing

Model 3. In Fig. 15 (e), A_1 and A_0 of M1 fluctuate above 4.5 and 3.5, respectively. A_2 fluctuates between 0 and 4.5. No continuous low points were observed. In Fig. 15 (f), A_1 of M2 stays above certain high value. A_2 stays high except for 1 point. A_0 shows larger fluctuations than those in the first two trials. The whole process went smoothly with no difficulties.

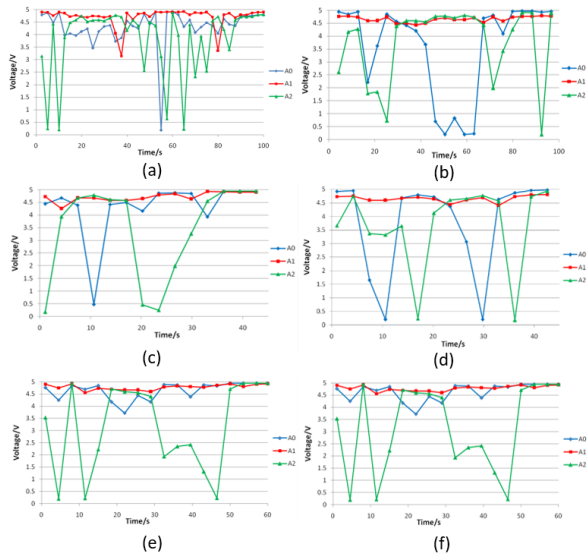


Figure 15. (a), (b), (c), (d), (e), and (f) are Sensor feedback of Testing Model trial 1, 2, and 3 of M1 and M2.

IV. DISCUSSION

The modular robotic system developed in this research combines modular robot with classic robotic control theory. Bluetooth communication capability is enabled for each module. It is applied to the field of colonoscopy, in which certain problems still exist, to try to improve it. As a result, a prototype with three independent modules were built and tested on a series of testing models, including one that partially simulates the sigmoid colon. By actually running the test, some significant details, feelings from the performer, and important observations are recorded. These details, feelings, and important observations are analyzed together with the numerical sensor and servo feedbacks. The evaluation results of the shape adjustment function are discussed in three main parts: the hardware and BT communication, the theoretical analysis, and the integrated practical performance.

A. Insertion Time Analysis

The purpose of measuring the insertion time in this research is to evaluate the stability of the insertion speed and its consistency using the shape adjusting function. For this purpose, the time is compared between trials and intervals rather than horizontally with devices in other research. To evaluate the insertion speed, there are difficulties that come from 2 main aspects. The system was inserted manually, thus, variations existed in the speed itself. No accurate numerical force feedback was used to control the speed. The speed only depended on the resistance force that was felt in the performer's hand.

To maximally assure the effectiveness of the data, the performer ran a number of trials before the real test to gain enough knowledge and stability for the process. The system was inserted in a particular and uniformed manner and Fig. 16 shows the average speed (AVG V), SD and CV in each 10 cm interval.

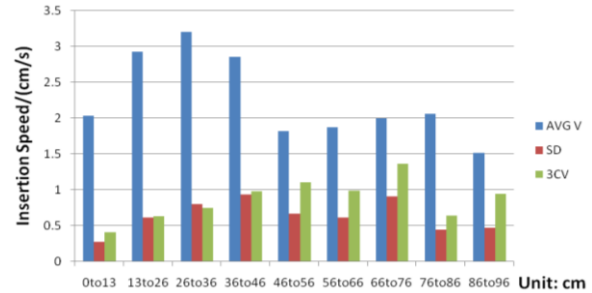


Figure 16. Average Insertion speed, standard deviation, and coefficient of variation of the 10 trials on Testing Model (Alpha Loop Sectionalized Insertion Speed/SD/CV)

The speed increases during the first 36 cm of insertion and reaches a maximum magnitude in the 26 to 36 cm interval. The first 13 cm of insertion is slow due to an obstructive edge at the beginning of the model for which the system must tilt up in order to overcome. Once the system has adjusted and bypassed the initial edge, the insertion becomes smoother with an insertion speed around 3 cm/s. When the system was inserted about 46 cm into the model, a significant increase of dynamic resistance was felt, decreasing the insertion rate to below 2 cm/s. This insertion distance corresponds to where the loop starts in the model. From 46 cm on, the force increased until the insertion was completed. In several cases, the system experienced forces that halted insertion, which are known as the static forces. Different from the dynamic force, which is mainly caused by the friction between the rubber shaft and the model's wall, static force is caused by the stalling of the system (mostly the distal part). The robotic system gets stuck somewhere in the model causing a dramatic increase of resistance. Most of the time the static force situation cannot be overcome by increasing the insertion force. The insertion speed fluctuate slightly around 2 cm/s from 46 to 86 cm of insertion, then it drops significantly to 1.5 cm/s from 86 to 96 cm. The reason is that there is a 3 to 4 mm lip bumping up at the end of the semi-rigid tube, which causes the unenclosed servo bracket of the system to get stuck on.

To evaluate the stability of the advancing speed, the coefficient of variation (CV) was calculated for each interval. Generally, the CV as the system is inserted from 0 to 76 cm. From 0 to 36 cm of insertion, the CV increases from 0.13 to 0.25. During the sharp bend in the testing model, which is roughly from 36 to 76 cm of insertion, the CV has values ranging from 0.33 to 0.45. The reason is that during these intervals, the system has a bigger chance of encountering static forces, which slows down the process. From 76 to 86 cm of insertion, the speed roughly stays the same and the CV is much smaller. This is because of the fact that the model becomes

straight after 76 cm. From 86 to 96 cm is where the system is about to come out of the model. The speed of the shape adjustment motion is sufficient for an acceptable advancing speed. To better control the speed, or robotize the insertion mechanism, force feedback is required.

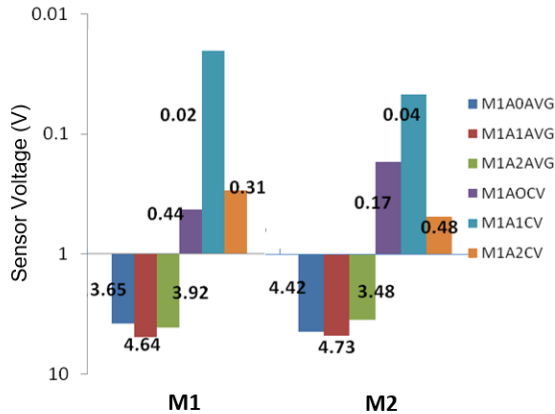


Figure 17. Statistic of sensor readings of M1 and M2

B. Sensor and Servo Feedback Analysis

By generally looking at the sensor data, regularity can be seen that each sensor in the same module behaves in a different way. Also, sensor data between different modules show great dissimilarities. Similarities are seen between trials on the same testing model. Figure 17 shows the statistics of M1 and M2's sensor data on the testing models. In the graph, M1A0AVG stands for the average reading of sensor A_0 in Module 1 for all three trials and M1A0CV stands for its coefficient of variation. Sensor A_1 's average value stays high and CV of A_1 shows slight variation, but no obvious trend is seen. A_2 shows a relatively low average value in the models and CV of A_2 stays roughly the model, and it is significantly larger than those of A_1 and A_0 .

The statistic analysis reflects general regularity of the sensor readings. Basically, the average reading represents the most likely and frequent distance (voltage) between the sensor and the wall during the process. The CV indicates the range of the adjustment (fluctuation). The cause of the fluctuation of the sensor readings is that the system attempts to adjust its shape during the process. All of the sensors have an average value that is larger than 3.0, which corresponds to a distance of 1 cm. Generally, the robotic system functions to adjust its shape according to the shape of the testing model. As suggested by the statistic analysis, among all the sensors, A_0 plays the most important role. The dramatic fluctuation of A_2 can be known as an evidence of the system functioning to avoid collision in X-Z plane (the vertical plane). The very slight fluctuation of A_1 exposed a defect of the hardware: the position of A_1 in the circumferential direction of the module should be adjusted so that it can come into play more effectively.

C. Hardware

The overall size and weight of each single module is impressive compare to those modular robots with similar

functions. The housing is able to hold all components together firmly during the whole insertion process. The servo bracket links the modules stably. The internal wirings are well protected. The sensor system is capable of locating the body of the system in a tubular environment. The arrangement of the servos allows the system to overcome sharp curves with smooth and continuous motion. The main achievement for the BT communication is that a mode is defined to allow multi-point communication between modules with point-to-point BT device. It is the key for wireless inter-module cooperation. The data transmission protocol can be programmed flexibly in Python. The one that developed for this research handled the heavy data flow stably and accurately during the whole process.

D. Practical Performance Evaluation

To present the evaluation results of the performance, the evaluation of the "evaluation method" needs to be stated. Testing Model was built with the intention of simulating the sigmoid colon and testing the function in a more realistic manner. The model was placed in an "alpha" shape, which simulates the "alpha loop" that happens frequently in the sigmoid colon. The material of the model was much more rigid than the actual colon so that it would not collapse, in which case, the robotic system would not be able to pass without compound operations. Generally, the testing model was realistic enough for the robotic system. During the insertion process, the performer controlled only the speed depending on the force felt in the hand. No other operations were done to insert the system. All ten trials performed on Testing Model succeeded. Real time pictures show efficiency of the shape adjustment function. Almost no skills were needed to finish this process. The motion of the system was smooth and continuous. Static forces were experienced in some cases mainly caused by the limitation of the hardware. The data flow protocol is capable for this function. Among tons of trials performed (no less than 100 trials), no data flow fault were encountered. The battery lasted about 25 to 30 minutes, during which 10 or more trials could be performed.

IV. CONCLUSION

In this study, a modular robotic system was developed and a prototype with three modules was implemented. Each module can process and communicate via Bluetooth independently. A sensor system with corresponding location logic is carried out for the shape adjustment function. Multi-point BT communication between modules and external PC is enabled. The data flow protocol can be defined flexibly. For the mathematical modeling, kinematic analysis (FK and IK) of the 5 degree of freedom system was implemented. A unique method that cooperates with the sensor system was used to determine the target position transformation matrix. The system succeeded in navigating itself through a testing model which has certain degree of randomness and the sense of reality. The skill that was required for finishing the insertion process was reduced. The size restriction needs to be solved for adapting more small components.

CONFLICT OF INTEREST

The authors declare no conflict of interest.

AUTHOR CONTRIBUTIONS

Liu analyzed the data, and wrote the paper; Choi guided and conducted the research; all authors had approved the final version.

REFERENCES

- [1] F. Cosentino, E. Tumino, G. R. Passoni, A. Rigante, R. Barbera, A. Tauro, and P. E. Cosentino, "Robotic colonoscopy," in *Colonoscopy*, 2011, pp. 291-308.
- [2] P. Boyle, and B. Levin, "World cancer report 2008," *International Agency for Research on Cancer Treat*, vol. 88, no. 1, pp. 123-132 (in Japanese), 2008.
- [3] P. Colquhoun, E. G. Weiss, J. Efron, J. J. Nogueras, A. Vernava, M., and S. D. Wexner, "Colorectal cancer screening: Do we practice what we preach," *Surgical Innovation*, vol. 13, no. 2, 81-85, 2006.
- [4] H. Messmann, "Atlas of colonoscopy: Techniques, diagnosis," *Interventional Procedures*, pp. 31-33, New York: Thieme, 2006.
- [5] T. Byers, B. Levin, D. Rothenberger, G. D. Dodd, and R. A. Smith, "American cancer society guidelines for screening and surveillance for early detection of colorectal polyps and cancer," *Update 1997. CA: A Cancer Journal for Clinicians*, vol. 47, no. 3, pp. 154-160.
- [6] D. K. Rex, D. A. Johnson, D. A. Lieberman, R. W. Burt, and A. Sonnenberg, "Colorectal cancer prevention 2000: Screening Recommendations of the american college of gastroenterology," *The American Journal of Gastroenterology*, vol. 95, no. 4, pp. 868-877, 2000.
- [7] N. M. Gatto, H. Frucht, V. Sundararajan, J. S. Jacobson, V. R. Grann, A. I. and Neugut, "Risk of perforation after colonoscopy and sigmoidoscopy: A population-based study," *Journal of the National Cancer Institute*, vol. 95, no. 3, pp. 230-236, 2003.
- [8] T. R. Levin, C. Conell, J. A. Shapiro, S. G. Chazan, M. R. Nadel, , and J. V. Selby, "Complications of Screening Flexible Sigmoidoscopy," *Gastroenterology*, vol. 123, no. 6, pp. 1786-1792, 2002.
- [9] W. S. Ng, S. J. Phee, C. Seow, and B. L. Davies, "Development of a Robotic Colonoscope," *Digestive Endoscopy*, vol. 12, no. 2, pp. 131-135, 2000.
- [10] K. J. Dowling, "Limbless locomotion: learning to crawl with a snake robot," (Doctoral Dissertation, NASA), 1996.
- [11] M. Yim, W. M. Shen, B. Salemi, D. Rus, M. Moll, H. Lipson, H. Lipson, E. Klavins, and G. S. Chirikjian, "Modular Self-reconfigurable Robot Systems [Grand Challenges of Robotics]," *Robotics & Automation Magazine, IEEE*, vol. 14, no. 1, pp. 43-52, 2007.
- [12] Wright, C., Johnson, A., Peck, A., McCord, Z., Naaktgeboren, A., Gianfortoni, P., Gonzalez-Rivero, M., Hatton, R., and Choset, H., 2007, October, "Design of a Modular Snake Robot," In *Intelligent Robots and Systems, 2007. IROS 2007. IEEE/RSJ International Conference on* (pp. 2609-2614). IEEE.
- [13] J. Denavit, and R. S. Hartenberg, "A kinematic notation for lower-pair mechanisms based on matrices," *Journal of Applied Mechanics*, pp. 215-221, 1955.
- [14] S. R. Buss, "Introduction to inverse kinematics with jacobian transpose, pseudoinverse and damped least squares methods," *IEEE Journal of Robotics and Automation*, vol. 17, pp. 1-19, 2009.
- [15] K. Grochow, S. L. Martin, A. Hertzmann, and Z. Popović, August, "Style-based Inverse Kinematics," In *ACM Transactions on Graphics (TOG)*, vol. 23, no. 3, pp. 522-531, ACM, 2004.
- [16] P. Valdastri, R. J. Webster, C. Quaglia, M. Quirini, A. Menciassi, and P. Dario, "A new mechanism for mesoscale legged locomotion in compliant tubular environments," *IEEE Transactions on Robotics*, vol. 25, no. 5, pp. 1047-1057, 2009.
- [17] M. Bourke, and D. Rex, "Tips for Better Colonoscopy from Two Experts," *American Journal of Gastroenterology*, vol. 107, no. 10, pp. 1467-1472, 2012.

Copyright © 2020 by the authors. This is an open access article distributed under the Creative Commons Attribution License ([CC BY-NC-ND 4.0](https://creativecommons.org/licenses/by-nc-nd/4.0/)), which permits use, distribution and reproduction in any medium, provided that the article is properly cited, the use is non-commercial and no modifications or adaptations are made.

Kaiquiang Liu earned M.S. degree in the Department of Mechanical Engineering, Ohio University. His research interests include robotics, microprocessor controller and medical devices.

JungHun Choi is an assistant professor of Mechanical Engineering, Georgia Southern University. His research interests are Biomedical Engineering, Design and development of Medical Devices and application.